

## Effect of Sputter Pressure on Zinc Oxide Thin Films deposited by RF Magnetron Sputtering

*Roger ONDO-NDONG, Hugues OMANA, Honoré GNANGA, and Hermance MOUSSAMBI*

Laboratoire pluridisciplinaire des sciences,  
Ecole Normale Supérieure,  
Libreville B.P 17009, Gabon

Copyright © 2018 ISSR Journals. This is an open access article distributed under the **Creative Commons Attribution License**, which permits unrestricted use, distribution, and reproduction in any medium, provided the original work is properly cited.

**ABSTRACT:** The objective of this research is to study the effect of sputter pressure on thin zinc oxide film deposited by RF magnetron sputtering technique on Si and glass substrates using ZnO disk with 99.99% purity. In order to avoid the effect of the thickness of the layers on the physical properties, we worked on samples of comparable thickness, from 0.8 to 1.1  $\mu\text{m}$ . The deposition is done with heating the substrate at very low temperature, which is currently the most favorable conditions for integration into a MEMS process. X-ray diffraction spectra showed that ZnO thin films are hexagonal wurtzite and exhibited a c-axis orientation of below  $0.32^\circ$  full width at half maximum of X-ray rocking curves. The preferential orientation is along the (002) direction reported for all ZnO samples deposited by sputtering RF magnetron. The general observation indicates that the parameters of the microstructure such as grain size, intrinsic stresses, dislocation density and the full width at half maxima (FWHM) dependent on the sputter pressure of the film. Sample deposited 3.35mTorr gives the best results. In addition, the transmission is more than 90% in the visible region. Ellipsometry data have been fitted with a Cauchy-Urbach model. From this fitting the refraction index (n), extinction coefficient (k) and thickness (d) of the sputtered ZnO films were determined. As a result of the combined spectroscopic ellipsometry, structural properties and transmission analysis, there was a good correlation in comparison. The network analyzer shows losses are -5dB at a  $k_{33} = 0.26$  experimental.

**KEYWORDS:** Thin films; X-ray diffraction; crystalline property; Transmittance; Ellipsometry; Electromechanic coupling coefficient.

### 1 INTRODUCTION

Over the last few decades, zinc oxide (ZnO) has been extensively studied because of its coexisting semiconductor, optical and piezoelectric properties [1]. ZnO has been found to be biocompatible [2] and has promising applications in surface acoustic waves, bulk acoustic waves, optical waveguides and filters due to its piezoelectric nature [3, 4]. Moreover, ZnO films must have a good crystalline quality, smooth and unconstrained for reliable and efficient devices. In view of these results, ZnO has been developed as a gas sensor [5], TCOs of solar cells [6], photocatalyst component [7] and as a light-emitting diode LEDs [8]. There are also SAW components that are not only used in the telecommunications sector, but also in the automotive, medical and industrial sectors [9, 10]. Other advanced applications such as components emitting UV light are based on pure ZnO have been developed. The spectral transmission and reflectance measurements are experimental methods most commonly used to obtain important information on the optical properties of ZnO. A good and useful way to obtain the parameters of the layer inside measurement is spectroscopic ellipsometry and reflectometry [11]. Using an appropriate model of the sample, one can obtain the values of many unknown variables by adjusting the measured data with the model parameters. The complex refractive index, the absorption coefficient, the energy of the bandgap, as well as the thickness of the layer may be provided using these methods. Several material models for spectroscopic ellipsometry exist in TCOs. Here, one of them: Cauchy-Urbach model is used. Several growth techniques are used for the production of thin films of ZnO [13-19]. It has also been found experimentally that the physical properties of ZnO thin films are sensitive to deposition conditions [20-22]. Among these techniques, radio frequency (RF) magnetron sputtering was more useful for uniform deposition over a large area of substrate

material. Indeed, it has been found experimentally that the physical properties of ZnO thin films are sensitive to deposition conditions [20-22]. In particular, during the growth of the films, the optimization of the sputtering pressure, as a method of improving their physical properties, may provide a way to control the growth rate, remove the defects and internal stress in the films. The sputtering pressure is a key parameter to improve the film quality and the device performance. The use of the optimum sputtering pressure has significant defects and stress in the ZnO films, thus changing their crystalline structure, optical transmittance, and band gap energy. Sputtering pressure has been reported to contribute to the fabrication of high quality films, the variation of stress, the shape of the crystalline grain, the lifetime of the charge carriers, and the conduction type of the materials [23]. Moreover it is also useful having good adhesion to the substrate, better reproducibility, high deposition rates and easy control of the composition of the films deposited using this technique. The properties of the RF magnetron sputter deposited films mainly depend on various deposition parameters for example substrate temperature, partial pressure of oxygen, sputtering power, sputtering pressure in the chamber, substrate bias voltage and thickness of the film. In this work, we made a systematic study of the physical properties of RF magnetron sputtered ZnO thin films as function of the sputtering pressure in the chamber. We presented new investigation results on zinc oxide (ZnO) thin film deposited on glass substrate using spectroscopic ellipsometer with a wavelength range from 400 nm to 900 nm. The measured ellipsometric data are fitted with theoretical spectra generated assuming appropriate models regarding the sample structures [24]. The fitting has been done by minimizing the squared difference between the measured and calculated values of the ellipsometric parameters ( $\Psi$  and  $\Delta$ ) and accurate information has been derived regarding the thickness and optical constants of the different layers. FWHM of the (002) x-ray rocking curve must be less than 0.32 for an effective electromechanical coupling [20-22].

## 2 EXPERIMENTAL MATERIALS AND METHODS

### 2.1 PREPARATION OF MATERIALS

The target used for fabrication of zinc oxide films was a cylindrical metallic zinc with 99.99% purity of 51 mm diameter and 6 mm thick. The metal target consisting only of zinc makes it possible to overcome the variation of the surface observed on thin films deposited with targets composed of several metals. Indeed, adjustments are necessary for the final composition of the deposited thin film. ZnO films were grown by rf magnetron sputtering on Si (100) 2-in wafers of p-type and glass (Corning 7059; USA) substrates at different sputtering pressure. Sputter pressure is the deposition pressure. The substrates were entirely cleaned with acetone using ultrasonic technique and dried before loading in the sputtering chamber. Magnetron sputtering was carried out in an oxygen and argon mixed gas atmosphere by supplying RF power at a frequency of 13.56MHz. The RF power was about 50W. The flow rates of both the argon and oxygen were controlled using flow meter (ASM, AF 2600). The sputtering pressure was varied by a Pirani gauge. Before deposition, the pressure of the sputtering system was under  $4.10^{-6}$  torr for more than 12h and were controlled by using an ion gauge controller (IGC – 16 F). We deposited an inking Ti/Pt on the silicon substrate in order to facilitate the adherence of ZnO films. Thin films were deposited on silicon, substrate under conditions listed in Table 1. These deposition conditions were fixed in order to obtain well-orientation zinc oxide films. The presputtering occurred for 30 min to clean the target surface. Deposition rates covered the range from 0.35 to 0.53  $\mu\text{m}/\text{h}$ . All films were annealed in a helium ambient at 650°C for 15mn.

*Table 1. Parameters deposition of ZnO by RF magnetron sputtering*

Samples	Pressure (mTorr)	Ratio O <sub>2</sub> %	Substrate (T°C)	Power (W)	Target-substrate (cm)	Time deposition (h)
ZnOT1	3.25	20	100	50	7	2
ZnOT2	3.30					
ZnOT3	3.35					
ZnOT4	3.40					
ZnOT5	3.45					

### 2.2 CHARACTERIZATION

In order to investigate the crystallographic properties of ZnO films, we carried out an X-ray diffraction. System used consists of a goniometer, an X-ray source producing copper K $\alpha$  radiation (CuK $\alpha$ ) with a wavelength  $\lambda = 0.154$  nm and a monochromator that eliminates K $\alpha$ 2 and K $\beta$  radiation [25]. The root-mean-square (rms) surface roughness of the films were characterized using an atomic force microscope (AFM). The optical absorption spectra are recorded between 300 and 900 nm wavelength using

UV-2550 UV-VIS Spectrophotometer at room temperature. The thicknesses of the films and the optical parameters (refractive index ( $n$ ) and extinction coefficient ( $k$ )) were determined with PHE 102 Spectroscopic Ellipsometry. To characterize the films, we use a HP 8752 A Network Analyzer whose bandwidth ranges from 300 KHz to 1.3 GHz. This type of device is one of instruments to define with precision the characteristics of an electrical circuit.

### 3 RESULTS AND DISCUSSION

#### 3.1 STRUCTURAL AND MORPHOLOGICAL PROPERTIES

Fig. 1 shows typical XRD patterns of ZnO thin films deposited on Si (100) orientation substrates at various sputtering pressure of 3.25, 3.30, 3.35, 3.40 and 3.45mTorr. Indeed, if we look at ZnO diagram, we notice on all samples, the presence of four peaks. Comparing the peaks with those of the ASTM file, we find that the peaks at  $34^\circ$  and  $38^\circ$  respectively represent the orientations according to the (002) and (101) planes of the ZnO films. On the other hand, the peaks at  $40^\circ$  and  $42^\circ$  respectively represent the direction along the plane (111) of the platinum and (003) titanium electrode.

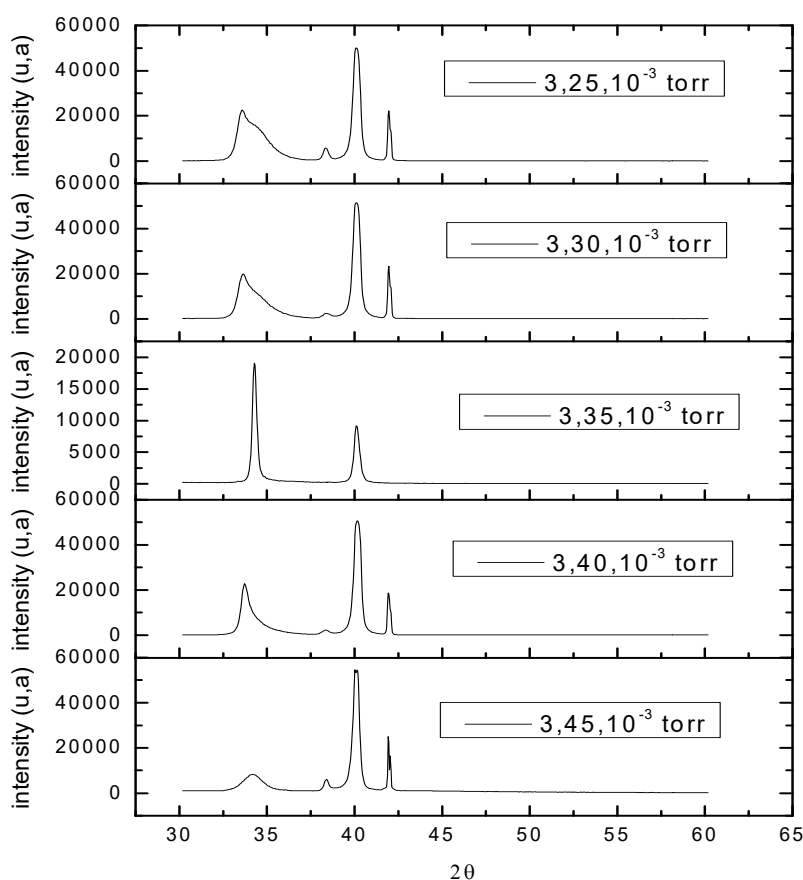


**Fig. 1. XRD patterns of ZnO thin films deposited at different sputter pressure**

Therefore, we can say that the deposited layers have a preferential orientation along the (002) plane. We find that the intensity of crystalline orientation of zinc oxide films varies with spray pressure. In addition, the deposited layer 3,35mTorr gives the best orientation by the intensity of the very high peak. Indeed, the ZnO layers preferentially grow along the axis c in the plane (002). Then, we proceeded to calculate the grain size of (002) plane for each sample from their respective X-ray diffraction spectra. The average crystallite sizes of the films deposited at different sputtering pressure have been estimated using the following Scherer formula [23]:  $D = \frac{k\lambda}{\delta \cos \theta}$  Where D is grain size, K is shape factor of a value having 0.94,  $\lambda$  is X-ray wavelength of the CuK $\alpha$  radiation ( $K=1.5418\text{\AA}$ ),  $\delta$  is full width at half maxima (FWHM) in radians and  $\theta$  is the Bragg's diffraction angle.

Indeed, grain size was calculated from this relationship. Previously, full width at half maxima (FWHM) of the diffraction peak and the diffraction angle corresponding to the (002) plane are determined from diffraction patterns of X-rays Fig. 2. We see a rapid increase in grain size between 3.25mTorr, 3.30mTorr 3.35mTorr. It goes from 20 to 44nm then a gradual decrease to 23nm when we increase the sputter pressure. This change is proportional to the evolution of full width at half maxima (FWHM) of the diffraction peaks. Indeed, we note that the development of the full width at half maxima (FWHM) depending on the substrate temperature reaches a minimum. This minimum was observed 3.35mTorr for value of 0.32°. Fig. 3 shows the evolution of the diffraction peak on the plane (002) of ZnO thin films synthesized under these experimental conditions. We observe that the intensity of the diffraction peak increases with the increase of the sputtering pressure to 3.35mTorr where it passes through a maximum, then the intensity decreases for the pressures higher than 3.35mTorr.

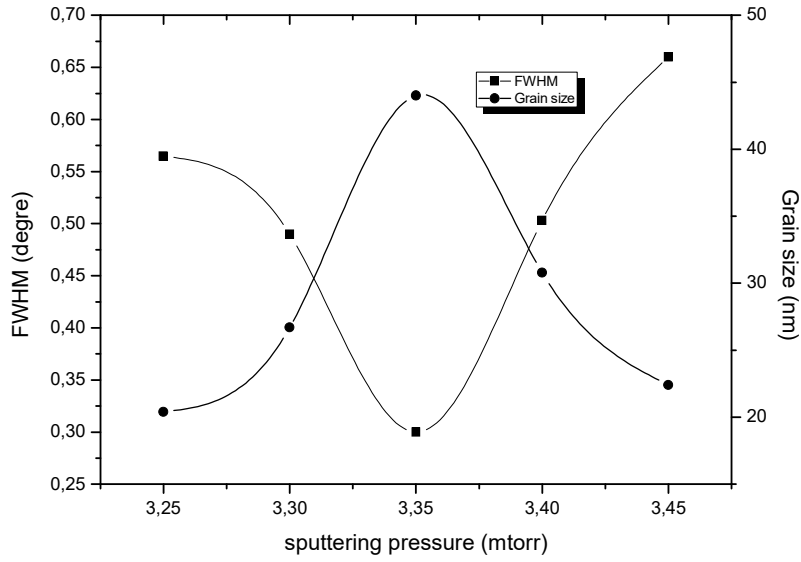


Fig. 2. Grain size of the ZnO films and the half-height width deposited at different sputter pressure

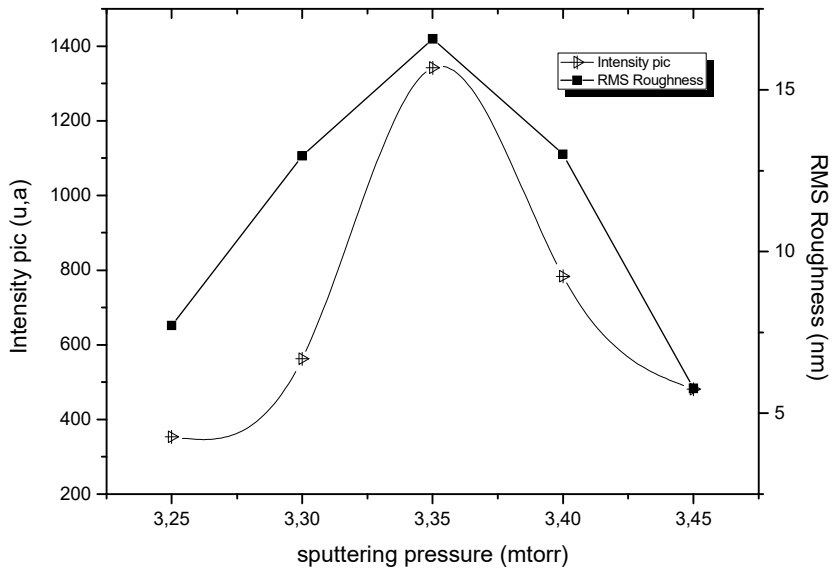


Fig. 3. The evolution of the diffraction peak on the (002) plane and surface roughness of ZnO thin films synthesized at different sputter pressure

This modification can be interpreted in that the partial increase of the sputtering pressure improves the crystallization of the grain ZnO films. However, the simultaneous combination of the increase of the sputtering pressure and the low temperature of the substrate leads to the formation of defects in the layer and may also lead to degradation of the structural quality of the films [26]. Thus, the 3.35mTorr sputtering pressure appears to be the optimal pressure for the growth of our ZnO thin films. A smooth surface is an essential property to avoid the dispersion of the physical properties in the ZnO films, but remains a handicap for the realization of MEMS. Indeed, it is necessary to have a fibrous appearance structure because the small crystals will be difficult to differentiate. But, with a sufficiently dense grain we can give the ZnO layer appropriate mechanical properties. The surface roughness of our layers was measured by AFM. Fig. 3 shows also the evolution of the roughness as a function of the sputtering pressure. We find that the surface roughness of our ZnO thin films varies with sputtering pressure. It increases gradually from 7 to 16nm when the sputtering pressure passes 3.25 to 3.35mTorr and decreases to 5.5nm when increases to 3.45mTorr. We can say that these results agree well with the results obtained with X-ray diffraction. The sample developed at 3.35mTorr has a very high intensity peak (002) confirming its high roughness compared to the other samples. We also noted the morphology of these samples by AFM. Fig. 4 shows the surface morphology of the films over an area (5  $\mu\text{m}$  x 5  $\mu\text{m}$ ). We can clearly observe the surface roughness of the samples. We note that the sample deposited 3.35mTorr shows the rougher surface, which confirms a good property for MEMS devices achievements.

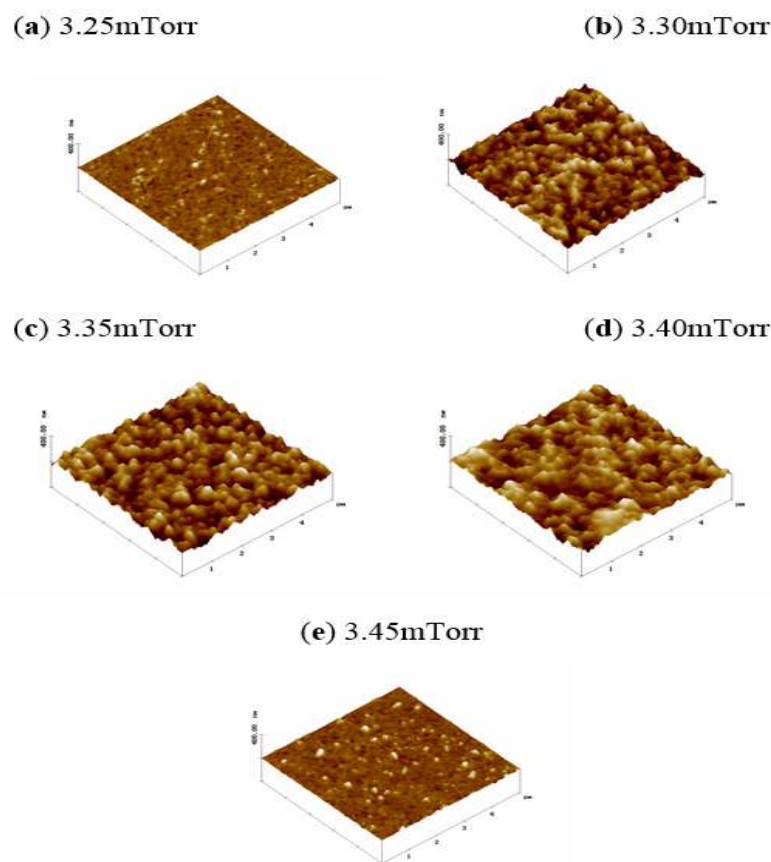


Fig. 4. AFM images with a scan of 0.4 x 0.4 $\mu\text{m}$  deposited ZnO films at different sputter pressure

### 3.2 STRESS PROPERTIES

All thin films deposited by RF magnetron sputtering have constraints. These constraints come from all processes related to the development of layers. They alter significantly the characteristics of mechanical strength, thermal or chemical involved predominantly, especially the phenomena of fatigue under stress. It therefore appeared necessary to us to make a quantitative study of residual stress of ZnO thin films prepared by RF magnetron sputtering. The stresses are evaluated by X-ray diffraction technique. The principle of the method is to determine the variation of the diffraction angle  $\theta$  of the stress layer with respect to the diffraction angle of the bulk material taken as reference. This parameter was obtained by operating the following equation [27]:

$$\Delta\sigma = -\frac{E_c}{\nu_c} \left( \frac{2\theta_{ref} - 2\theta}{2\theta} \right)$$

$E_c$  is Young's modulus of zinc oxide with  $E_c = 2,11 \times 10^{11} \text{ N.m}^{-2}$  [28],  $\nu_c$  is Poisson's ratio of ZnO with  $\nu_c = 0.36$  [28],  $2\theta_{ref}$  and  $2\theta$  are, respectively, the angles of diffraction peaks of (002) planes of the ASTM reference and ZnO thin films deposited. Dislocation density ( $\gamma$ ) have been calculated using the crystallite size of the film [29-31]:

$$\gamma = \frac{1}{D^2}$$

Fig. 5 shows the evolution of intrinsic stresses and dislocation density in ZnO samples that have almost identical thicknesses.

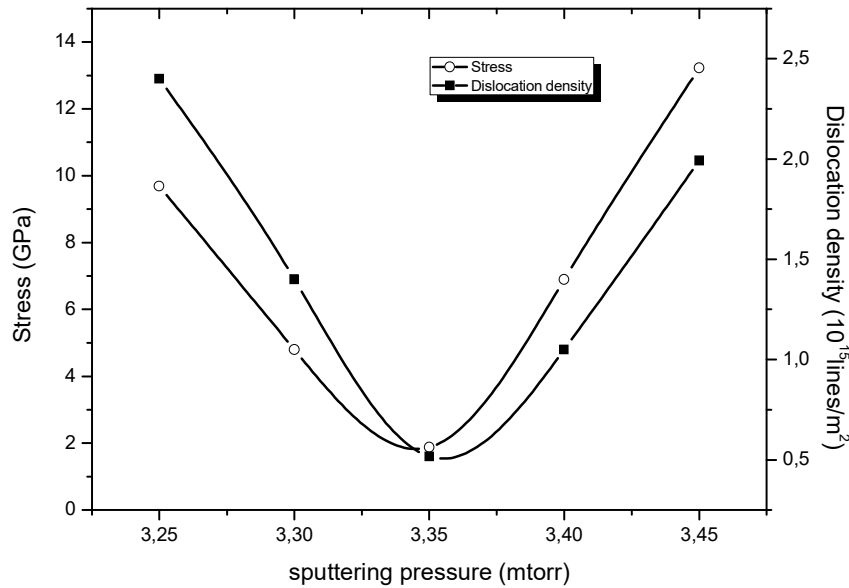


**Fig. 5. Evolution of intrinsic stresses and the dislocation density in the ZnO samples**

All these samples have compressive stresses ranging from  $9,365 \times 10^{13}$  to  $4.5 \times 10^{13} \text{ N/cm}^2$ . These stresses are due to the presence of nanograins which the crystal lattice has interstitial defects [32, 33]. On the other hand, the evolution of these stresses is a function of different sputtering pressure. These stresses are minimal for samples deposited at 3.35mTorr compared to other samples. The result is identical with respect to the dislocation density. This shows that these intrinsic stresses are related to the coalescence dynamics of the grains. A small-grain material offers many limitations for the realization of electronic devices and promotes the development of micro-stresses, themselves caused by growing defects. This explains the high residual stress values in samples other than those deposited at 3.35mTorr. These limitations are thought to be mainly due to the Hoffman [34] grain boundary relaxation phenomenon to explain the presence of stress stresses in polycrystalline thin films after deposition.

### 3.3 TRANSMITTANCE

In order confirm the values of deposition parameter which seem to give the best result from a structural point of view, we have studied optical properties in order to respond to the influence of sputtering pressure. As we want to avoid the effect of thickness of layer on optical properties, we have worked on samples whose thicknesses are between 0.8 and 1.1  $\mu\text{m}$ . We could not use silicon substrate because the bandgap energy value ( $E_g = 1.1\text{eV}$ ) makes absorbing structure to UV radiation from the source of spectrometer. So we used glass (Corning 7059; USA) substrates. The rough surface or materials with inhomogeneity in volume generates low signal. Thus, it is necessary to make an adjustment, before any measurement: 100% for the transmittance of Pyrex substrate taken as reference. Piloting, digital capture and processing of data is performed by a microcomputer. Measuring the light transmission through a dielectric film parallel face, in the working range considered, is sufficient to determine the real and imaginary parts of the complex refractive index and the thickness. Wales et al [35] and Lyashenko et al [36] have developed a method using successive approximations and interpolations to calculate these three

quantities. Manificier et al. [37] have developed a method, like in the same range of applicability but differs from Lyashenko by its precision. Fig. 6 shows the transmission spectra of ZnO thin films deposited at different sputtering pressure. We observe that the transmission spectra are high (40% to 90%) for all samples. We note that the sample of ZnO developed 3.35mTorr has a maximum transmission of about 90%. By cons, for samples prepared at higher pressures to 3.35mTorr, transmission spectra are not exploitable. And those deposited at pressures below 3.35mTorr present very low transmission between 40 and 60%. These observations confirm results obtained by X-ray diffraction where we found that the samples are poorly crystallized and that the grain size is unusually small compared to that obtained with the sample developed 3.35mTorr. It is also observed that the absorption front at a wavelength for which the transmission spectra is reduced to 50% is around 375-400 nm. The difference of the extrema of the samples prepared at pressures lower than or equal to 3.35mTorr is maximum 100°C. Subramanyam et al. [38] confirm these results. In fact, they get an order of 86% transmittance and observed a decrease in optical transmission with the temperature range 300-400°C.

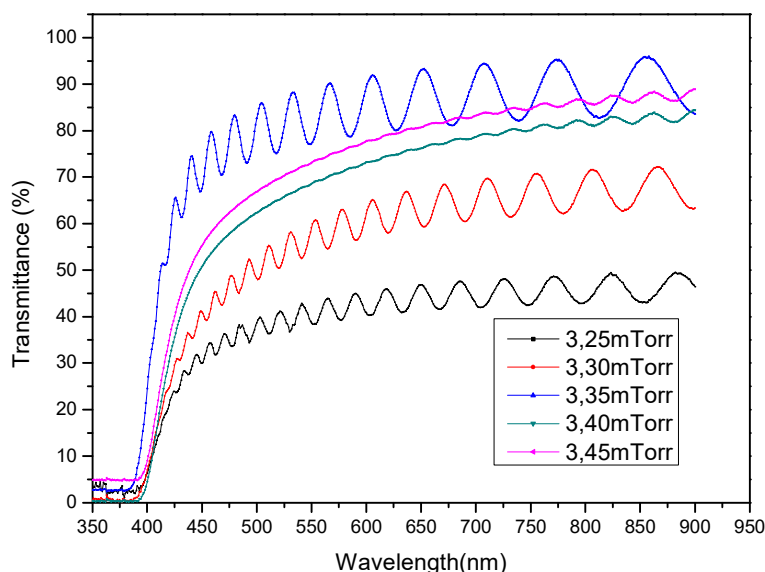


Fig. 6. Transmittance spectra of ZnO films deposited at different sputter pressure

The variations of the refractive index as a function of the different wavelengths for different sputter pressure were calculated. The index ranges from 1.65 to 2.1. The refractive index has a high dispersion for developed films at sputter pressures above 3.40mTorr and below 3.30mTorr.

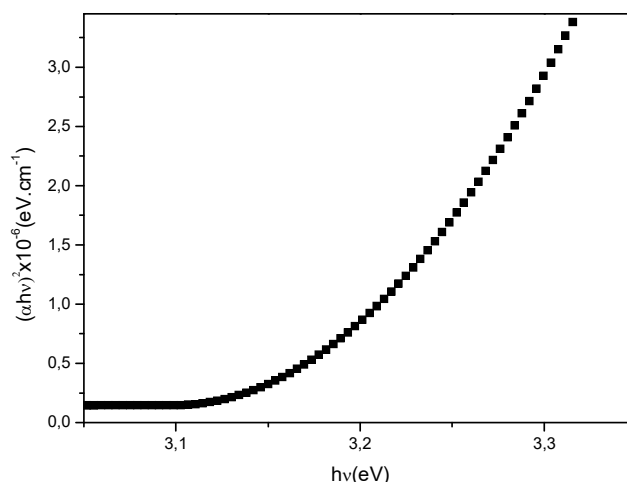


Fig. 7.  $(\alpha h\nu)^2 \propto h\nu$  plots for ZnO thin films

Comparing these results to those obtained by X-ray diffraction where we observed that the preferred orientation of the sample developed 3.35mTorr is (002) plane and its full width at half maxima (FWHM). This may indicate that the variation of the refractive index with the sputtering pressure can be accompanied by a change of the grain size in the growth direction. Bachari obtained, depending on the temperature, the full width at half maxima of the same order of magnitude as those of our samples with the corresponding refractive index ranging from 1.8 to 2.1 [39]. We observed a decrease of the refractive index of ZnO films at high sputtering pressure.

The optical band gap energy ( $E_g$ ) of the films was calculated by using optical method. The  $(\alpha h\nu)^2 \propto h\nu$  variation graph of ZnO thin films was plotted as shown in the inset of Fig 7. This study is carried out on the sample deposited 3.35mTorr.

The linear dependence of  $(\alpha h\nu)^2$  on  $h\nu$  at higher photon energies indicates that the grown ZnO films have essentially direct-transition-type semiconductors. Extrapolation of the linear portions of  $(\alpha h\nu)^2$  to zero gave the value of  $E_g$ . Fig. 7 shows the graph of  $(\alpha h\nu)^2$  vs. photon energy  $h\nu$  for the ZnO films deposited at 3.35mTorr sputtering pressure. The estimated band gap values  $E_g$  is 3.15 and are in good agreement with those published by different authors for ZnO films deposited with sputtering, and are close to the reported one for the single crystal form [40-42]. Indeed, it is well-known that the energy band gap of a semiconductor is affected by the residual strain, defects, charged impurities, disorder at the grain boundaries [43], and also particle confinement. If the films have less thickness and a smaller grain size, the widening of the respective conduction and valence bands will be less, and this results in a wider energy gap [44].

### 3.4 CHARACTERIZATION BY SPECTROSCOPIC ELLIPSOMETRY

To optimize the quality of materials used in the optoelectronic components, it is very useful to study the optical parameters of these materials. Also, the analysis of the ZnO thin films by ellipsometric spectroscopic (SE) was carried out. Determined the thickness, the refractive index ( $n$ ) and the extinction coefficient ( $k$ ). SE measures the change in polarization state of incident light and gives ellipsometric parameters known as  $\Psi$  and  $\Delta$ , which are related to the complex reflection coefficients with the equation:

$$\rho = \frac{\tilde{R}_p}{\tilde{R}_s} = \tan(\Psi) \cdot e^{i\Delta}$$

where  $\tilde{R}_p$  and  $\tilde{R}_s$  are complex reflection coefficients which are parallel and perpendicular to the plane of incidence, respectively [45]. Ellipsometric data were fitted using Cauchy-Urbach equations. These equations are given as:

$$n(\lambda) = A_n + \frac{B_n}{\lambda^2} + \frac{C_n}{\lambda^4} \text{ and } k(\lambda) = A_k e^{B_k(E-E_b)}$$

where  $A_n, B_n, C_n$  are Cauchy parameters and  $A_k, B_k$  are Urbach parameters.

Fitting the experimental ellipsometric spectra of  $\Psi$  allowed the determination of the film thickness ( $d$ ), of the sample thin films deposited at 3.35mTorr. The experimental data were analyzed by using Cauchy-Urbach model. The thicknesses determined by fitting the experimental ellipsometric spectrum. Ellipsometric spectrum is shown Figure 8 and the best-fit model parameters of ZnO thin films are listed in Table 2.

**Table 2. Thicknesses and Spectroscopy Ellipsometry data of ZnO thin films**

Film	Thickness (nm)	$A_n$	$B_n \text{ (nm)}^2$	$C_n \text{ (nm)}^4$	$A_k$	$B_k \text{ (eV)}^{-1}$	MSE
ZnO	800	2.42	0.1	0.02	0.08	1.34	0.1

The quality of the fit can be judged by the mean square error (MSE) defined as [46]:

$$MSE = \left\{ \frac{1}{2N - M} \cdot \sum_i (\Psi_m^i - \Psi_c^i)^2 + (\Delta_m^i - \Delta_c^i)^2 \right\}^{\frac{1}{2}}$$

Where N is the total number of experimental observations (in SE measurements, there are two observations,  $\Psi$  and  $\Delta$ , for each chosen wavelength). M is the number of fitting parameters, and the subscripts m and c represent the measured and the calculated data, respectively, where  $i$  is used to sum over all of the measurements.

Refractive index, extinction coefficient of ZnO film on glass were studied as a function of wavelength. The simulation  $n$ , as a function of the wavelength is shown in Figure 8, with the fitting parameters that are listed in Table II. One can see the

experimental refractive index curve from 1.9 to 2.2. This corresponds to a relatively large deviation of  $\Psi$  and  $\Delta$  in the same range which comes from the strong absorption of ZnO interband transition. It can be seen in Figure 9 the extinction coefficient  $k$  having non-zero values. It can be seen that  $k$  may be regarded as zero in the range of 750 to 850 nm, although there are small perturbations that are supposed to originate from the dispersion to the back of the glass substrate. These results are in agreement with literature.

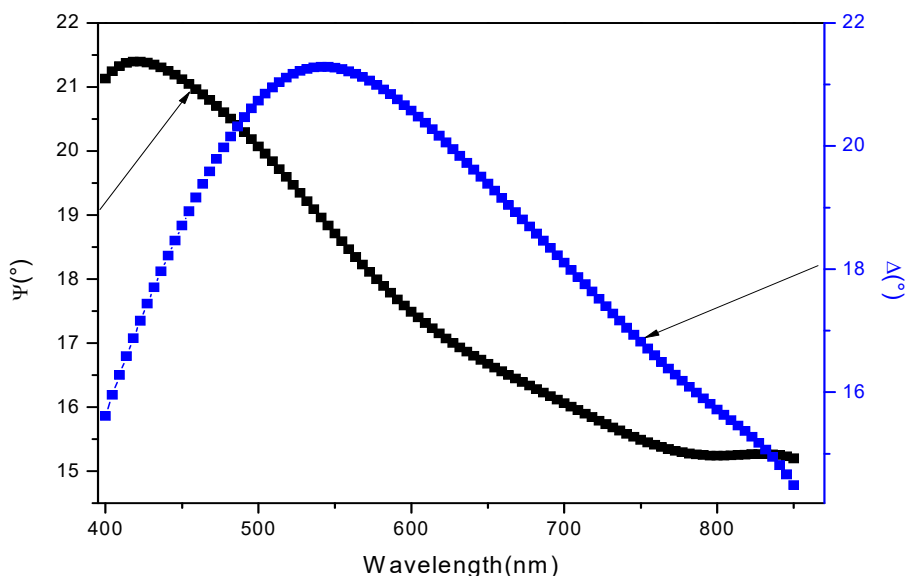


Fig. 8.  $\Psi$  and  $\Delta$  spectral of ZnO thin films

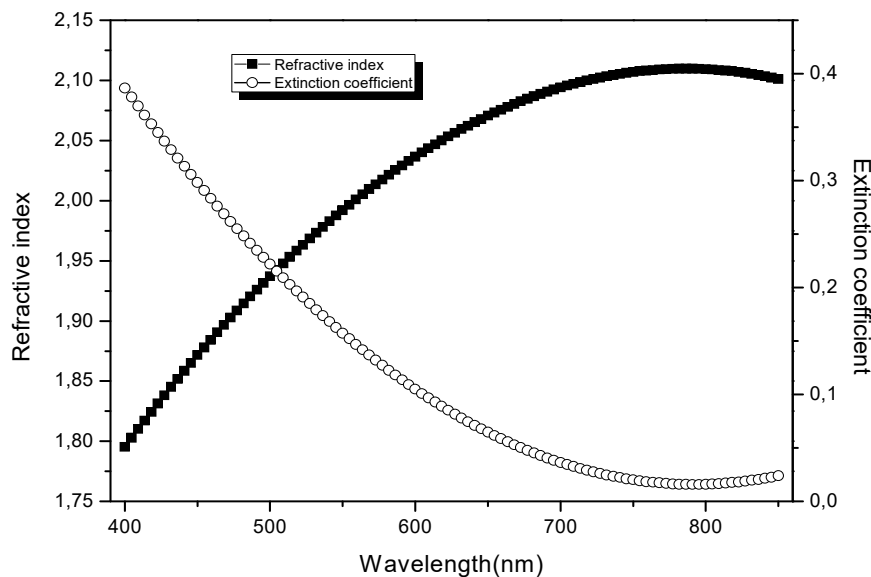


Fig. 9. Refractive index and extinction coefficient spectral of ZnO thin films

### 3.5 ELECTROMECHANICAL COUPLING COEFFICIENT

In a piezoelectric solid, the propagation of an elastic wave with wave vector is governed by an eigen value equation called Christoffel equation [18]:

$$\Gamma_{ik} u_k = \rho V^2 u_i$$

Dans un solide piézoélectrique, la propagation d'une onde élastique de vecteur d'onde  $\vec{k}$  est régie par une équation aux valeurs propres appelée équation de Christoffel :

Which  $u_i$  are the components of the displacement,  $\rho$  is the density of the solid and  $\Gamma_{ik}$  the tensor Christoffel

$$\Gamma_{ik} = \left( C_{ijkl}^E + \frac{e_{uij}e_{vkl}n_u n_v}{\epsilon_{rs}^S n_r n_s} \right) n_j n_l$$

The resolution of the Christoffel equation leads to three real and positive eigen values corresponding to propagation speeds of three waves. They are obtained by solving:

$$|\Gamma_{ik} - \rho V^2 \delta_{ik}| = 0$$

The wave propagates along the z direction. The Christoffel tensor in the case of a piezoelectric material:

$$\Gamma = \begin{vmatrix} C_{44} & 0 & 0 \\ 0 & C_{44} & 0 \\ 0 & 0 & C_{33} + \frac{e_{33}^2}{\epsilon_{33}} \end{vmatrix}$$

We therefore obtain an active piezoelectric longitudinal wave speed

$$V_3 = \sqrt{\frac{C_{33} + \frac{e_{33}^2}{\epsilon_{33}}}{\rho}}$$

This wave propagates along the c- axis ZnO thin films. Speed of longitudinal waves of the order of 6330 m/s. The electromechanical coupling coefficient is defined as:

$$k_{33} = \frac{e_{33}}{\sqrt{\epsilon_{33} C_{33} + e_{33}^2}}. \text{ This allows us to calculate and find } k_{33} = 0.3$$

We performed a microwave characterization of the developed ZnO thin films in order to measure the electromechanical coupling coefficient and the piezoelectric activity. Indeed, we know that the network analyzer generates wave trains, such as an instantaneous electromotive force generator and a frequency  $f$ . We worked in reflection. This technique is used to evaluate the efficiency with which the transducer converts electrical activity into mechanical activity and vice versa.

We characterize the sample obtained with a spray pressure of 3.35mtorr.

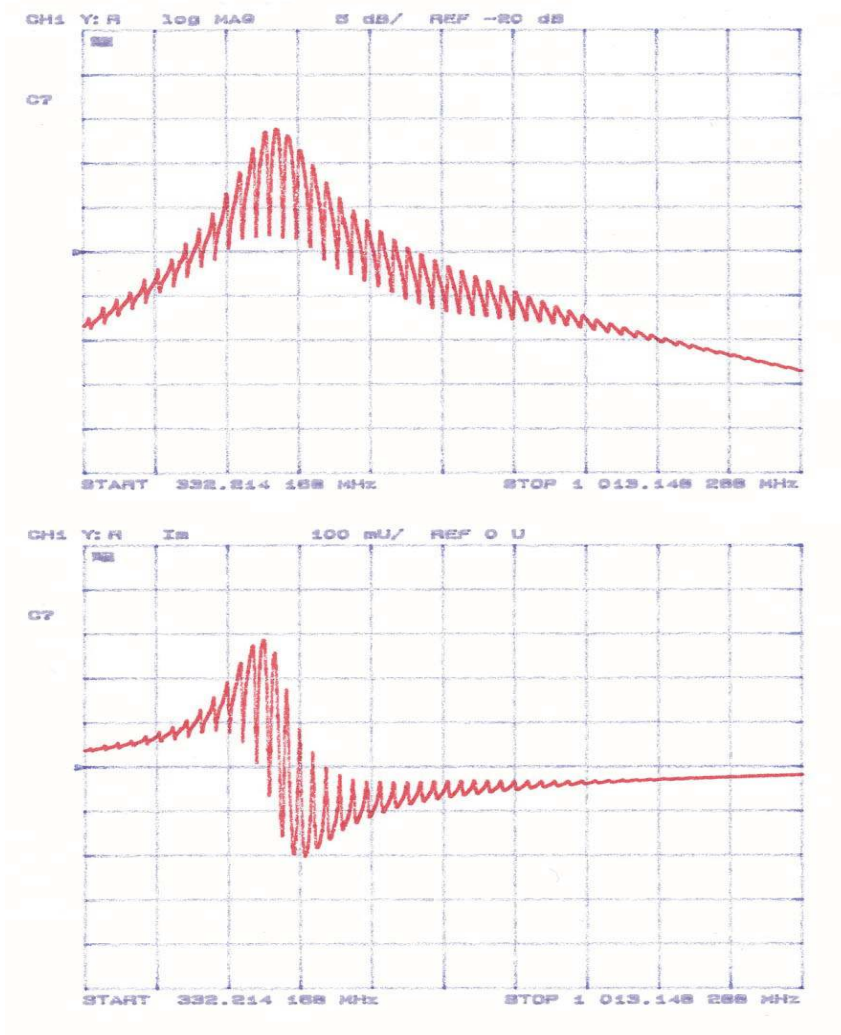


Fig. 10. Electrical admittance of ZnO resonator with losses.

Fig. 10 shows the variation of the real and imaginary parts of the electrical admittance of the frequency. We observe a variation of the electrical admittance at the input of the resonator and the appearance of oscillations at the input of the resonator. These oscillations are superimposed on the general envelope. These oscillations are due to the propagation medium. They reflect the changes in the real and imaginary parts of the measured electrical admittance. This means that the system reacts to the electric charge with a delay effect. Indeed, the shape of the curves shows that there is interference of the waves propagating in the propagation medium that is the silicon substrate.

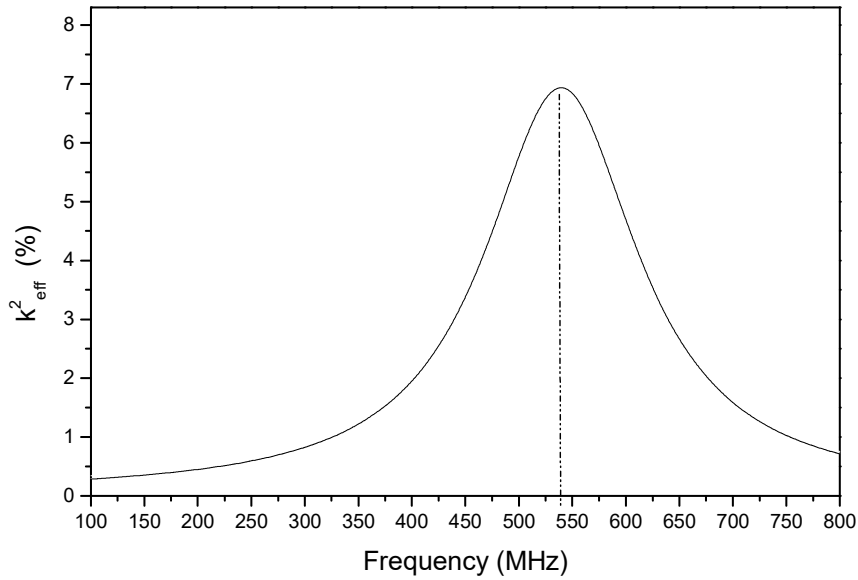


Fig. 11.  $k_{eff}^2$  function of frequency

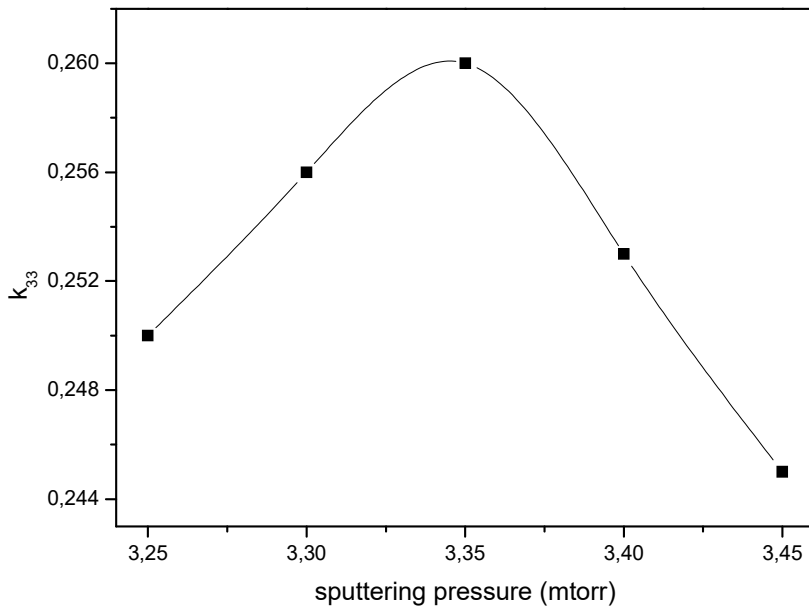


Fig. 12. Electromechanical coupling coefficient at different sputtering pressure.

To determine the coupling coefficient of the structure, one places oneself at the fundamental resonance of the resonator that is to say at the frequency where the real part of the admittance is maximum and the minimum susceptance.

We observe in Fig. 11 the value of coupling coefficient reaches a maximum when the number of modes of propagation in the thickness of the substrate is the highest. The maximum propagation mode observed is the fundamental mode of propagation of ZnO. We obtain a coupling coefficient  $k_{eff} = 0.26$ . This value is of the order of 92% of the theoretical value. Indeed, we deduce electric losses of the order of 0.4% in the substrate and 0.4% in the ZnO layer. This is because the speed of propagation of the wave in these media is complex.

Fig. 12 shows the evolution of coupling coefficient of ZnO thin film for different pressures sputter. These curves follow the same variation in the intensities of the peaks (002) also as a function of the different spray pressures. We get the value close to 0.26, which corresponds to 92% of the theoretical value. This result is substantially equal to that obtained by the network analyzer

#### **4 CONCLUSION**

In conclusion, the best quality ZnO films in terms of crystal structure have been deposited on a silicon and glass substrates in 3.35mTorr sputtering pressure by RF magnetron sputtering with metallic zinc target. X-ray diffraction shows that the films are preferentially oriented along the c-axis in the plane (002) normal to the substrate plane. We note that the development of the full width at half height (FWHM) as a function of the temperature of the substrate reaches a minimum. This minimum was observed at 3.35mTorr for a value of 0.32°. At the same time, the roughness reaches a maximum of 16nm. All of ZnO thin films deposited by RF magnetron sputtering have compressive stress. The crystallographic characteristics correlated with the transmission more than 90% to confirm the results obtained 3.35mTorr. Therefore, the structural properties and high optical transparency of the thin zinc oxide layer oriented well can be deposited successfully by rf magnetron sputtering. Moreover, ZnO films, deposited on glass substrate by rf magnetron sputtering, have been analyzed based on spectroscopic ellipsometry in compare with transmission spectroscopy from a UV-IS system. Ellipsometry data have been fitted with a Cauchy-Urbach model of ZnO film. As a result of the combined spectroscopic ellipsometry and transmission analysis, there was the good correlation in comparison. The evolution of the electromechanical coupling coefficient of the ZnO thin films for the different spray pressures confirms the variation of the intensities of the peaks (002). The experimental results are in agreement with the theoretical law.

#### **REFERENCES**

- [1] Fahoume M., Maghfoul O., Aggour M., Hartiti B., Chraibi F. and Ennaoni A., Growth and characterization of ZnO thin films prepared by electrodeposition technique, *Sol. Energy Mater. Sol. Cells.* 90, pp. 1437–1444, 2006.
- [2] Patel NR, Gohil PP., A review on biomedical: scope, applications & human anatomy significance, *Int. J. emerg. Teechnol. Adv. Eng.*, 2(4), pp. 91-101, 2012.
- [3] O. Legrani, O. Elmazria, S. Zhgoon, P. Pigeat, A. Bartasyte, Packageless AlN/ZnO/Si Structure for SAW Devices Applications, *IEEE Sensors Journal*, Vol. 13(2), pp.487-491, 2013.
- [4] Sofian M. Kanan, Oussama M. El-Kadri, Imad A. Abu-Yousef and Marsha C. Kanan, Semiconducting Metal Oxide Based Sensors For Selective Gas Pollutant Detection, *Sensors*, 9, pp. 8158-8196, 2009.
- [5] H.-W. Ryu, B.-S. Park, S.A. Akbar, W.-S. Lee, K.-J. Hong, Y.-J. Seo, D.-C. Shin, J.-S. Park, G.-P. Choi, ZnO sol-gel derived porous film for CO gas sensing, *Sens. Actuator, B* 96, pp. 717-722, 2003.
- [6] D. Kim, H. Kim, Self-textured transparent conductive oxide film improves efficiency of solar cells, *Proc. of SPIE* 7603, pp. 76030G-1-76030G-8, 2010.
- [7] E.S. Elmolla, M. Chaudhuri, Degradation of amoxicillin, ampicillin and cloxacillin antibiotics in aqueous solution by the UV/ZnO photocatalytic process, *J. Hazard. Mater.*, 173, pp. 445-449, 2010.
- [8] J.Y. Lee, J.H. Lee, H.S. Kim, C.-H. Lee, H.-S. Ahn, H.K. Cho, Y.Y. Kim, B.H. Kong, H.S. Lee, A study on the origin of emission of the annealed n-ZnO/p-GaN heterostructure LED, *Thin Solid Films*, 517, pp. 5157-5160, 2009.
- [9] S. Krishnamoorthy, A.A. Iliadis, Properties of high sensitivity ZnO surface acoustic wave sensors on SiO<sub>2</sub>/(100) Si substrates, *Solid-State Electronics*, 52, pp. 1710-1716, 2008.
- [10] [17] Y.C. Lin, C.R. Hong, H.A. Chuang, Fabrication and analysis of ZnO thin film bulk acoustic resonators, *Appl. Surf. Sci.*, doi:10.1016/j.apsusc.2007.11.059, 2007.
- [11] Lennart Fricke, Tammo Böntgen, Jan Lorbeer, Carsten Bundesmann, Rüdiger Schmidt-Grund, Marius Grundmann, An extended Drude model for the in-situ spectroscopic ellipsometry analysis of ZnO thin layers and surface modifications, *Thin Solid Films*, 571, Part 3, pp. 437-441, 2014.
- [12] L.R. Damiani and R. D. mansano, Zinc oxide thin films deposited by magnetron sputtering with various oxygen/argon concentrations, *journal of Physics: conference series* 370, pp. 012019, 2012.
- [13] M. G. Faraj and K. Ibrahim, Optical and Structural Properties of Thermally evaporated Zinc oxide Thin Films on polyethylene terephthalate Substrates, *International Journal of Polymer Sciences*, volume 2011, Article ID 302843, pp. 1-4, 2011.
- [14] E. Muchuweni, T. S. Sathiaraj, H. Nyakoty, Effect of gallium doping on the structural, optical and electrical properties of zinc oxide thin films prepared by spray pyrolysis, *Ceram. Int.* 42, pp. 10066-10070, 2016.

- [15] Toshiyuki Kawaharamura, Hiroyuki Nishinaka and Shizuo Fujita, Growth of Crystalline Zinc Oxide Thin Films by fine-Channel-Mist Chemical vapor Deposition, Japanese Journal of Applied Physics, Volume 47, number 6R, pp. 4669-4675, 2008.
- [16] Z. L. Wang and J. Song, Piezoelectric nanogenerator based on zinc oxide arrays, Science. 312, pp. 242-246, 2006.
- [17] R. Baraki, N. Novak, T. Fromling, T. Granzow, and J. Rodel, Bulk ZnO as piezotronic pressure sensor, App. Phys. Lett. 105 (11) (2014) 111604-111604-4.
- [18] Y.Q. Fu, J.K. Luo, X.Y. Du, A.J. Flewitt, Y. Li, G.H. Markx, A.J. Walton, and W.I. Milne, Recent developments on ZnO films for acoustic wave based bio-sensing and microfluidic applications: a review, Sensors and Actuators B. 143 (2010) 606-619.
- [19] Wei Long Liu, Yan Chang Chang, shu Huei Hsieh, Wen Jauh Chen, Effects of Anions in electrodeposition Baths on morphologies of zinc Oxide Thin Films, Int. J. electrochem. Sci., 8, pp. 983-990, 2013.
- [20] D.R. Sahu., Studies on the properties of sputter-deposited Ag-doped ZnO films, Microelectron. J. 38, pp. 1252-1256, 2007.
- [21] Li X, Shen R, Zhang B, dong X, Chen B, Zhong H, Chen L, Sun J, Du G., Nitrogen doped ZnO thin films prepared by photo-assisted metal-organic chemical vapor deposition, j Nanosci Nanotechnol. Nov 11(11), pp. 9741-4, 2011.
- [22] Roshchina NM, smertenko PS, Stepanov VG, Zavyalova LV, Lytvyn OS., Some properties of thin films structures on the base of ZnO obtained by MOCVD method, Solid State Phenomena, Vol. 200, pp. 3-9, 2013.
- [23] Fang-Hsing Wang, Jen-Chi Chao, Han-Wen Liu and Tsung-Kuei Kang, Physical Properties of ZnO Thin Films Codoped with Titanium and Hydrogen Prepared by RF Magnetron Sputtering with Different Substrate Temperatures, Journal of Nanomaterials, Volume 2015, Article ID 936482, pp. 1-11, 2015.
- [24] Y.W.Heo, D.P. Norton and S.J. Pearton. Zinc Oxide Bulk, Thin Films and nanostructures, J. Appl. Phys. 98, pp. 073502-073508, 2006.
- [25] Annual book of ASTM Standards (2001).
- [26] M. I. Khan, K. A. Bhatti, Rabia Qindeel, Leda G. Bousiakou, Norah Alonizan, Fazal-e-Aleem, Investigations of the structural, morphological and electrical properties of multilayer ZnO/TiO<sub>2</sub> thin films deposited by sol-gel technique, Results in physics, 6, pp. 156-160, 2016.
- [27] S.Mridha and D.Basak, Effect of thickness on the structural, electrical and optical properties of ZnO films, Mater. Res. Bull. 42, pp. 875-882, 2007.
- [28] Han M.Y.,and Jou J.H. Detennination of the mechanical properties of rf magnetron sputtered zinc oxide thin films on substrates. Thin Solid Films, 260, pp 58-64, 1995.
- [29] Fahoume M., Maghfoul O., Aggour M., Hartiti B., Chraibi F. and Ennaoni A. Growth and characterization of ZnO thin films, Energy Mater. Cells. 90, pp. 1437-1444, 2006.
- [30] T. P. Rao and M. C. Santhoshkumar, Physical properties of Ga-doped znO thin films by spray pyrolysis, Journal of Alloys and Compounds, 506, pp. 788-793, 2010.
- [31] J.B.Seon, S. Lee, J.M. Kim and H.D. Jeong, Spin-coated CdS thin films for n-channel thin films trnasistors, Chem. Mater., 21, pp. 604-611, 2009.
- [32] R. Hong, J. Shao, H. He, Z. Fan, Influence of buffer layer thickness on the structure and optical properties of ZnO thin films, Appl. Surf. Sci., 252, pp. 2888-2893, 2006.
- [33] Hur T.B., Hwang Y.H., Kim H.K., Lee I.J., Strain effects in ZnO thin films and nanoparticles, J. Appl. Phys., 99, pp. 064308, 2006.
- [34] R.W. Hoffman, Stresses in thin films: The relevance of grain boundaries and impurities, Thin Solid Films, 34, pp 185-190, 1976.
- [35] J. Wales, G.J. Lovitt and R. A. Hill, Optical properties of germanium films in the 1-5  $\mu$  range, Thin Solid Films., 1, pp. 137-150, 1967.
- [36] S.P. Lyashenko and V.K. Miloslavski, A simple method for the determination of the thickness and optical constants of semiconducting and dielectric layers, Opt. Spectrosc., 16, pp. 80-81, 1964.
- [37] J.C. Manifacier, J. Gasiot and J.P. Fillard, A simple method for the determination of the optical constants  $n$ ,  $h$  and the thickness of a weakly absorbing thin film, J. Phys. E: Sci. Instrum., 9, pp. 1002-1004, 1976.
- [38] T. K. Subramanyam, B. S. Naidu, S. Uthana, Physical Properties of Zinc Oxide Films Prepared by DC Reactive Magnetron Sputtering at Different Sputtering Pressures, Cryst. Res. Technol., Vol. 34(8), pp. 981-988, 1999.
- [39] K. Laurent, D.P. Yu, S. Tusseau-Nenez and Y Leprince-Wang, Thermal annealing effect on optical properties of electrodeposited ZnO thin films, journal of Physics D: Applied Physics, vol. 41(19), pp. 195410, 2008.
- [40] T. Prasada Rao, M.C. Santhosh Kumar, S. Anbumozhi angayarkanni, M. Ashok, Effect of stress on optical band gap of ZnO thin films with substrate temperature by spray pyrolysis, Journal of Alloys and compounds, 485, pp. 413-417, 2009.
- [41] Ning Tang, Jin Liang Wang, Heng Xing Xu, HongYong Peng, Chao Fan, Optical characterization of ZnO thin films deposited by RF magnetron sputtering method, Science in china serie E: Technological sciences, volume 52, issue 8, pp 2200-2203, August 2009.

- [42] A. Ismail, M. J. Abdullah, The structural and optical properties of ZnO thin films prepared at different RF sputtering power, *Journal of King Saud University-Science*, volume 25, issue 3, pp 2009-2015, July 2013.
- [43] Jamilah Husna, M. Mannir Aliyu, M. Aminul Islam, P. chelvanathan, N. Radhwa Hamzah, M. Sharafat Hossain, M.R. Karim, Nowshad Amina, Influence of Annealing Temperature on the Properties of ZnO Thin Films Grown by Sputtering, *Energy Procedia*, 25, pp. 55-61, 2012.
- [44] N.Ehrmann and R. Reineke-Koch, Ellipsometric studies on ZnO:Al thin films: Refinement of dispersion theories, *Thin Solid Films*, Vol. 519,n°4, pp. 1475-1485, 2010.
- [45] Y. Yang, X.W. Sun, B.J. Chen, C.X. Xu, T.P. Chen, C.Q. Sun, B.K. Tay and Z. Sun, Refractive indices of textured indium tin oxide and zinc oxide thin films, *Thin Solid Films*, Vol., 510, n°1-2, pp. 95-101, 2006.
- [46] Q.H. Li, D. Zhu, W. Liu, Y. Liu and X.C. Ma, Optical properties of Al-doped ZnO thin films by ellipsometry, *Appl. Surf. Sci.*, 254, pp. 2922-2926, 2008.
- [47] D. Royer, E. Dieulesaint, *Ondes élastiques dans les solides*, Tome 2, ed. Masson, 1996.